PUMMA

Research and Innovation Action (RIA)

This project has received funding from the Euratom research and innovation programme 2019-2020 under Grant Agreement No 945022

Start date : 2020-10-01 Duration : 54 Months

PuMMA
Plutonium Management for More Agility

New correlation law for melting temperature of MOX fuels

Authors : C. Gueneau (CEA), P. Fouquet-Métivier (CEA), M.M. Desagulier (CEA), L. Vlahovic (JRC), G. Nicodemo (Polimi), D. Robba (JRC), D. Staicu (JRC), P. Martin (CEA), J. Martinez (CEA), D. Pizzocri (Polimi), L. Luzzi (Polimi), N. Chauvin (CEA).

PUMMA - Contract Number: 945022

Project officer: Renata BACHORCZYK-NAGY

Document title	New correlation law for melting temperature of MOX fuels
Author(s)	C.Gueneau (CEA), P. Fouquet-Métivier (CEA), M.M. Desagulier (CEA), L. Vlahovic (JRC), G. Nicodemo (Polimi), D. Robba (JRC), D. Staicu (JRC), P. Martin (CEA), J. Martinez (CEA), D. Pizzocri (Polimi), L. Luzzi (Polimi), N. Chauvin (CEA).
Number of pages	33
Document type	Deliverable
Work Package	WP3
Document number	D3.6
Issued by	CEA
Date of completion	2025-05-07 14:09:32
Dissemination level	Public

Summary

This work was carried out as part of WP3 on ?Fuel properties with high Pu content: Measurements and modelling?, dedicated to the assessment of the main properties of irradiated and non-irradiated MOX fuel, in order to reduce significantly sources of uncertainty in the safety evaluation. In Task 3.3, thermodynamic properties of the fuel are evaluated. In this work, all available experimental data on fresh (U,Pu)O2±x oxides from the literature and measured in frame of the ESNII+, ESFR-SMART and PUMMA projects are reviewed. Data were measured using conventional thermal analysis or advanced laser heating techniques. Based on the analysis of uncertainties, a selection of experimental data is proposed. Data calculated using the CALPHAD model recently published by Fouquet-Métivier et al. [Fou23] are compared to these experimental data. Finally the data are used as input to derive a new correlation law for fresh fuel, to be used in Fuel Performance Codes.

Approval

Date	By
2025-05-16 08:22:00	HÓzer ZOLTáN (MTA EK)
2025-05-28 15:15:57	Nathalie CHAUVIN (CEA)

Disclaimer

Table of contents

List of figures

This project has received funding from the Euratom research and training programme 2019-2020 under grant agreement No 945022.

List of tables

This project has received funding from the Euratom research and training programme 2019-2020 under grant agreement No 945022.

Abbreviations and Acronyms

Acronym	Description
WP	Work Package
CALPHAD	CALculation of PHAse Diagram
EPMA	Electron Probe Micro-Analysis
ESFR-SMART	European Sodium Fast Reactor Safety Measures Assessment and Research Tools
ESNII+	European Sustainable Nuclear Industrial Initiative
HERFD-XANES	High Energy Resolution Fluorescence Detected – X-ray Absorption Near Edge Structure
INSPYRE	Investigations Supporting MOX Fuel Licensing in ESNII Prototype Reactors
JAEA	Japan Atomic Energy Agency
JRC	Joint Research Center
MAE	Mean Absolute Error
MAPE	Mean Absolute Percentage Error
MOX	Mixed Oxide Fuel
O/M ratio	Oxygen to Metal ratio
RLS	Reflected Light Signal
SOL-GEL	SOLution-GELation
TAF-ID	Thermodynamics Advanced Fuels – International Database
XAS	X-ray absorption spectroscopy
XRD	X-Ray Diffraction

This project has received funding from the Euratom research and training programme 2019-2020 under grant agreement No 945022.

Summary

This work was carried out as part of WP3 on "Fuel properties with high Pu content: Measurements and modelling", dedicated to the assessment of the main properties of irradiated and non-irradiated MOX fuel, in order to reduce significantly sources of uncertainty in the safety evaluation. In Task 3.3, thermodynamic properties of the fuel are evaluated.

In this work, all available experimental data on fresh $(U,Pu)O_{2\pm x}$ oxides from the literature and measured in frame of the ESNII+, ESFR-SMART and PUMMA projects are reviewed. Data were measured using conventional thermal analysis or advanced laser heating techniques. Based on the analysis of uncertainties, a selection of experimental data is proposed.

Data calculated using the CALPHAD model recently published by Fouquet-Métivier *et al.* [Fou23] are compared to these experimental data. Finally the data are used as input to derive a new correlation law for fresh fuel, to be used in Fuel Performance Codes.

Keywords

MOX fuel, margin to fuel melting, solidus temperature, correlation law, CALPHAD

This project has received funding from the Euratom research and training programme 2019-2020 under grant agreement No 945022.

1. Introduction

The fuel melting behaviour establishes a fundamental safety restriction on the margin to fuel melting, which must be respected for safe operation and thermodynamic stability of the fuel under irradiation, both under normal and transient conditions. A pin design for fast reactor application must be optimized and assessed considering this limit and the high operative temperatures foreseen. The aim of this work is to provide a new correlation law for the melting temperature data of fresh $(U_{1-y}Pu_y)O_{2\pm x}$ fuel with y=Pu/(U+Pu) and x, the deviation to the ideal oxygen stoichiometry of 2.

Extensive experimental campaigns were carried out using conventional thermal analysis at JAEA in 2005-09 [Mor05,Kat08,Kat09] and later at JRC Karlsruhe using advanced laser heating technique as part of European ESNI++ [Mar17,Sta17], ESFR-SMART [Mik17] and PUMMA [Mar25] projects, as well as thermodynamic modelling of the U-Pu-O system using the CALPHAD method, improved as part of INSPYRE project [Fou23].

In this work, all the experimental data are reviewed. The uncertainties are discussed and a selection of experimental data is proposed. The most recent CALPHAD model is then compared with these experimental data. Finally a new correlation law is derived using these selected experimental data as input data.

2. Review of experimental melting data

A critical review of melting temperature data from the literature for $(U,Pu)O_{2\pm x}$ mixed oxides was published in 2009 by Kato [Kat09], mainly based on the measurements made at JAEA by conventional thermal arrest technique. Recently, in 2023, Fouquet-Métivier *et al.* [Fou23] also did a review of the experimental data including measurements by both conventional thermal analysis and advanced laser technique. On this basis, the authors modified the CALPHAD model of Guéneau *et al*. [Gue11] for the liquid phase.

Extensive melting temperature measurement campaigns have been performed by Manara *et al.* [Man05,Man08], De Bruycker *et al.* [Deb10,Deb11A,Deb11B], Böhler *et al.* [Boh14], Strach *et al.* [Str16], Fouquet-Métivier *et al.* [Fou22B] (ESNII+ [Mar17,Sta17] and ESFR-SMART [MiK17] projects) and Desagulier [Des23] (PuMMA project [Mar25]) by laser heating technique. In this section, all experimental data measured by both techniques are reviewed. Uncertainties are discussed and a selection of data is proposed, as input for a new correlation law.

This project has received funding from the Euratom research and training programme 2019-2020 under grant agreement No 945022.

2.1 Conventional thermal arrest technique

Kato [Kat09] reviewed existing melting temperature measurements made by conventional thermal analysis. The most recent studies using this technique were carried out at JAEA [Mor05,Kat08,Kat09]. Samples were heated in an induction furnace. Several capsule geometries were tested [Kat08]. Initially, W capsules sealed in vacuum by electron beam welding were used. The temperature of the sample was measured using a pyrometer placed at the bottom of the capsule. The heating rate was of 40-80 K/min. Thermal arrests were observed in heating curves. Standards materials (Al_2O_3, Nb, Mo, Ta) were used to calibrate the temperature. Uncertainty was estimated at ± 35 K.

Mixed oxides samples containing up to 100 % PuO_2 were studied. The samples were synthesized by sintering at 1973 K for 3 hours in an atmosphere of Ar / 5 % H_2 with added H_2O. The O/M ratio was adjusted by annealing the samples at 1023 K for 5 hours at $\Delta G(O_2)$ = -400 kJ/mol. The homogeneity of the samples was checked using XRD and EPMA. It is not clear how the authors determined the initial O/M ratio of the samples whose uncertainty is not given. The authors claim that it does not change during the tests because the samples are in a closed system (capsule). However, there is a free volume in the capsule that may allow vaporization of the samples. This phenomenon is not reported by the authors although large porosities are observed by SEM, which could be explained by vaporization. After the tests, the samples were characterized by XRD and EPMA. The final O/M of the samples was not determined.

The authors demonstrated that a chemical interaction occurred between the samples and the W crucible at high Pu contents, leading to underestimated melting temperatures. This important observation showed that all previous measurements made with W crucible in the 60s and 70s were unreliable. At that time, the authors did not characterize the samples after the tests to check the possible sample/crucible interaction. Re crucibles were therefore tested [Kat08].

The melting point of UO_2 was found to be 3133 ±14 K by the author, in good agreement with the measurement of Manara *et al.* (3123 K) [Man05].

Measurement was trickier for PuO_2 due to its high oxygen potential relative to UO_2. In this case, the authors observed a reaction with the W or Re capsule [Kat08].

Using an ideal solid solution model between UO_2 and PuO_2, Kato estimated the melting temperature of PuO_2 at 2839 K. The author considered a linear decrease of the melting temperature with Pu content in the mixed oxide. A measurement was made for $PuO_{1.76}$ showing a possible maximum of the solidus temperature of 3031 K for which no crucible interaction was observed.

For $(U,Pu)O_2$ samples, a reaction with the W crucible was observed by the author for samples containing more than 30% Pu. The use of a Re capsule improved measurements for high Pu contents.

This project has received funding from the Euratom research and training programme 2019-2020 under grant agreement No 945022.

Using their selected experimental data, Kato *et al.* [Kat09] derived a solid solution model of the UO_2-PuO_2-$PuO_{1.7}$ system to predict solidus/liquidus temperatures for $(U,Pu)O_{2\pm x}$ mixed oxides.

It can be concluded that measurements using the conventional thermal arrest method [Kat09] can only be selected:

- for Pu contents below y=0.3 when W crucible have been used
- for Pu contents up to y=0.6 when Re crucibles have been used.

Regarding the influence of the O/M ratio, the results show that from an O/M ratio close to 2, the solidus/liquidus temperature increases as the O/M decreases. This suggests the existence of a maximum in the liquidus temperature, corresponding to the congruent melting temperature, for an O/M ratio lower than 2, close to 1.9, that is not well known.

2.2 Advanced laser heating technique

The laser heating technique used by Manara *et al.* [Man05,Man08], De Bruycker *et al.* [Deb10,Deb11A,Deb11B], Böhler *et al.* [Boh14], Strach *et al.* [Str16] and in the PhD. of P. Fouquet-Métivier [Fou22,Mar17,Sta17,Mik17] and M-M. Desagulier [Des23,Mar25] is presented.

2.2.1 Experimental setup

In order to avoid possible crucible-sample interactions, a laser heating technique was developed in the last decades at Joint Research Centre-Karlsruhe (Germany). The schematic representation of the setup is illustrated in Figure 1 .

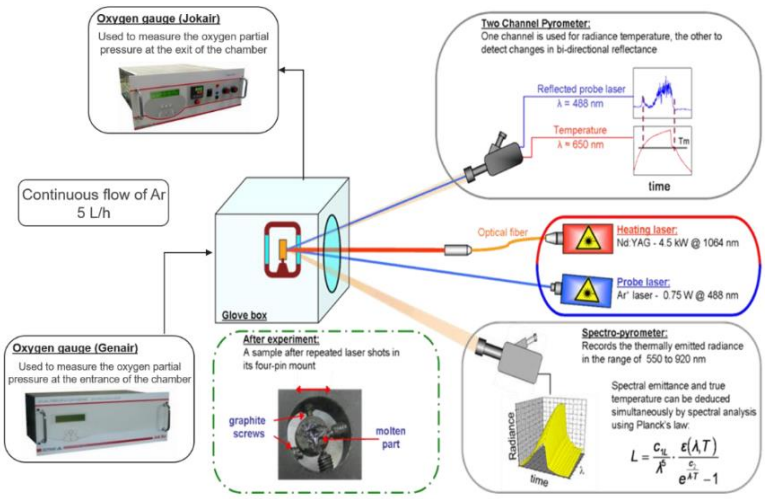

Figure 1 – Schematic representation of the laser heating setup.

To perform the experiment, disks or squares of the pellets of approximatively 1-1.5 mm thickness were first cut and then held by means of graphite screws in a graphite sample holder. The sample holder was then placed into an airtight autoclave, flushed by a flow (5 $L.h^{-1}$) of gas (Argon or Argon+6.5 $\%H_2$) with an overpressure of 0.3 MPa to avoid vaporization.

This project has received funding from the Euratom research and training programme 2019-2020 under grant agreement No 945022.

2.2.2 Solidus/Liquidus temperatures measurements

A 4.5 kW Nd:YAG continuous wave laser operating at 1064 nm was used to emit a short pulse (500 ms) of 200-250 W, focusing on a circular beam of 3 mm on the sample surface. The radiance temperature T_λ at the sample's surface was measured using a fast two-channel pyrometer operating near 650 nm, with a bandwidth of 27 nm and a nominal measurement spot size of 0.5 mm in diameter. This temperature corresponds to the one measured by a pyrometer calibrated in terms of blackbody radiance (emissivity equal to unity). The other channel of the pyrometer (488 nm) is used to detect changes in bi-directional reflectance using the RLS (Reflected Light Signal) technique, as a second method for the determination of the phase transitions.

For some samples, a 256-channel pyrometer was used to determine the emissivity and detect the surface emissivity variations during the melting/freezing experiments. A focusing unit is used to collect the radiation emitted by the sample surface, and to channel it into an optical fiber directly connected to the integrated spectrometer. In some cases, due to technical issues, the normal spectral emissivity of the samples could not be assessed experimentally. The emissivity of 0.83 ± 0.05 was then chosen, as experimentally determined for UO_2 and PuO_2 respectively by Manara *et al.* [Man05] and De Bruycker *et al.* [Deb10]. This value is also consistent with the emissivity measured in previous works on $U_{1-y}Pu_yO_2$ mixed oxides by De Bruycker *et al.* [Deb11B], Böhler *et al.* [Boh14], Strach *et al.* [Str16] and in the PhD. of M-M. Desagulier [Des23].

In some cases, to minimize thermal shocks and ensure the thermomechanical stability of the pellet, pre- and post-heating steps were performed at 1700 K. In addition, between four to nine successive shots were performed for some samples to improve the quality of the thermogram, to assure a good repeatability of the measurements and allow an easier determination of the solidus temperature.

The temperature of the phase transitions was determined by analysis of the thermal arrests in the cooling curve of the recorded thermogram. The true temperature is corrected based on the emissivity and transmittance, as explained in [Fou22,Des23].

Uncertainties on the measured temperature were estimated according to the propagation error law [Man08], taking into account the uncertainty associated to the calibration of the pyrometer, the emissivity and the transmittance of the optical system. With a coverage factor k=2, the cumulative uncertainty was estimated to be ± 30 K at 3000 K for $U_{1-y-z}Pu_yAm_zO_{2\pm x}$, *i.e.* ± 1 % of the recorded temperature.

2.2.3 Oxygen partial pressure measurements

Recently, the laser heating setup used at JRC-Karlsruhe was improved by the installation of two oxygen gauges, at the chamber inlet and outlet, to measure the oxygen partial pressure inside the autoclave during measurements under

This project has received funding from the Euratom research and training programme 2019-2020 under grant agreement No 945022.

argon or air [Cas24]. At each shot, a peak in oxygen partial pressure was observed corresponding to either absorption or release of oxygen in the sample during the shot. Knowing the initial O/M ratio of the samples and integrating the number of moles of oxygen over time for each peak, it was then possible to determine the changes in O/M ratio of the samples after each shot. This setup was used in the PhD. of P. Fouquet-Métivier [Fou22] and M-M. Desagulier [Des23] to assess and quantify the change in the O/M ratio of $(U,Pu)O_{2\pm x}$ samples along the shots for the first time.

The measurement of the oxygen partial pressure was performed every 3 s at the chamber outlet. The residual oxygen content of the atmosphere was measured in the gas, ranging from $pO_2 \approx 10^{-6}\ atm$ in Ar to $pO_2 \approx 10^{-26}\ atm$ in Ar + 6.5 % H_2. After each shot, the sample was allowed to cool down so that the atmosphere restabilized to its residual value. A shift in the detection of the peak of the pO_2 was observed compared to the moment at which the laser shot was performed. Indeed, the latter lasted 500 ms while the oxygen partial pressure was measured every 3 seconds. In addition, waiting steps ranging from 30 min to 2.5 hours were required for the oxygen partial to stabilize at its residual value. The time to record pO_2 was therefore much longer than the time taken to perform the shots. This means that only the value of O/M at room temperature before and after the shot could be determined. No information on the change in the O/M ratio at high temperature during the shots, and specifically where the solidus temperature was measured, could be deduced. The O/M at room temperature after the last shot was chosen as sample O/M ratio corresponding to the measured solidus temperature.

Further explanations on the detailed steps in determining the O/M ratio from pO_2 variations can be found in [Cas24,Fou22,Des23]. In this work, the uncertainty on the resulting O/M ratio was of ± 0.01.

2.3 Uncertainties

Uncertainties mainly concern:

- The measured temperature corresponding to the thermal arrest.

In general, a thorough understanding of measurement systems, particularly those employed for the determination of melting temperature is imperative to ensure precision and reliability in research outcomes. This is especially crucial to mitigate additional uncertainties, such as those associated with the pellet/crucible interaction, to ensure the integrity and validity of the experimental results.
The melting of $(U_{1-y}Pu_y)O_{2\pm x}$ mixed oxides is usually non congruent in the investigated O/M range (O/M>1.92). A solidification interval exists with a solid in equilibrium with a liquid phase. However, in most of the cases, a single thermal arrest is detected. The measurement could therefore correspond to the solidus or liquidus temperature. The measured temperature is usually considered as the solidus temperature, based on phase field simulations performed by Welland in [Boh14]. However more

This project has received funding from the Euratom research and training programme 2019-2020 under grant agreement No 945022.

systematic simulations of this type are needed, to confirm that the measured temperature corresponds to the solidus, in which the interaction between the gas and the sample should be considered to reproduce the thermogram and assess the O/M change of the sample as a function of temperature. In addition, supercooling and segregation phenomena during solidification could lead to a deviation between the real solidus temperature and the measured one.

- The O/M ratio at the measured temperature.

As already discussed in the previous sections, the O/M ratio at high temperature cannot be determined. Therefore, to reduce the uncertainties, it is mandatory to have as much as possible information on the samples, at least, the initial and final O/M ratio of the samples. It is imperative to gain a full understanding of the manufacturing process, including its characteristics and the raw materials used. Detailed knowledge of the structural and microstructural properties of the samples is essential. This includes an understanding of the experimental methods used to determine properties such as cationic homogeneity, density, O/M, and others.

It is evident that these factors can significantly impact the level of uncertainty. A review of the selected data reveals that, in some cases, information are limited. Consequently, all data from literature that fail to meet the required level of precision and detail for the previous points will be excluded from the subsequent selection.

2.4 Selection of experimental data

This section presents a summary of the selected data, followed by an initial comparison. The selection of data was based on the degree of accuracy available in the melting measurement itself, on the material and its structural and microstructural properties, and on the post-melting analyses. The selected data are summarised in Table 1.

Among the data measured using conventional thermal analysis, the data of Kato *et al.* [Kat09] are the only selected ones for the following reasons. As reported in section 2.1, the homogeneity of the samples was checked using XRD and EPMA. For the temperature measurements, the authors used conventional thermal analysis, with an estimated uncertainty of ± 35 K. It is not clear how the authors determined the initial O/M ratio of the samples. However, the authors are the only ones to have investigated a wide range of O/M ratio between 1.92 and 2 and the absence of interaction between the sample and the crucible was systematically checked. Therefore the data of Kato *et al.* measured in samples containing up to 60 % Pu are selected. For higher Pu contents, the data are discarded due to an interaction with the crucible.

This project has received funding from the Euratom research and training programme 2019-2020 under grant agreement No 945022.

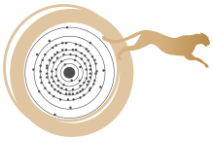

De Bruycker *et al.* [Deb11b] performed the first laser heating tests on $(U,Pu)O_2$ samples. Later, Böhler *et al.* [Boh14] and Strach *et al.* [Str16] carried out additional measurements with the same technique. Only the data measured by Böhler *et al*. [Boh14] are selected because the authors have improved the quality of the measurements and performed phase field simulations to interpret the results. Moreover the authors made extensive characterizations of the samples before and after the laser shots.

The samples studied by Böhler *et al* [Boh14] were prepared by sintering. In order to determine the initial O/M ratio, XRD was performed after manufacturing. Different values were obtained depending on the samples (±0.01): O/M = 2.00 for y = 0, 0.03 and 0.90, O/M = 1.99 for y = 0.25, 0.50, O/M = 1.98 for y = 0.40 and O/M = 1.97 for 0.09. Small changes of the O/M ratio were observed after melting for some samples thanks to post-melting characterizations using Raman spectroscopy, XRD and XAS.

The same laser setup was used in the most recent studies by Fouquet-Métivier [Fou22] and Desagulier [Des23]. All samples were manufactured by co-milling except for y = 0.45 which was prepared by SOL-GEL. After synthesis, the samples were extensively characterized using a multi-scale characterisation strategy. By this way, the initial structural and microstructural properties of the samples are well known. This reduces the uncertainty associated with the samples composition. The O/M ratio determined before were obtained by HERFD-XANES with the following uncertainty: ± 0.01. The uncertainty of the solidus temperature is ±30 K (section 2.2.1.1); however, a larger uncertainty of ± 50 K is taken as ± 30 K appears to be low (~1%) for such high temperature measurement. Finally, the O/M ratio of the melting pool was estimated by two technics: using oxygen partial pressure gauges (section 2.2.1.2) and by HERFD-XANES. The associated uncertainty is 0.01. All the data measured by Fouquet-Métivier [Fou22] and Desagulier [Des23] are selected.

In order to provide a comprehensive overview of the experimental data, the selected temperature data are plotted as a function of the Pu content (y) for fixed O/M ratio of 2.00, 1.99, 1.98, 1.97 (Figure 2– a,b,c,d).

Starting from pure UO_2, a decrease in the melting temperature is observed as the Pu content increases up to y=0.6. A minimum in the melting temperature is observed at 2950 K for a Pu content around y=0.65 and O/M=1.98-1.99. For higher Pu contents, the melting temperature increases up to pure PuO_2.

There is a good overall consistency between the experimental data. It can be noticed that the solidus temperature data of Böhler et al [Boh14] are systematically a lower than those of Kato [Kat09] and Fouquet-Métivier [Fou22].

A representation of the data as a function of the O/M ratio for different Pu contents will be given in the next section, where the models are presented.

This project has received funding from the Euratom research and training programme 2019-2020 under grant agreement No 945022.

Table 1. Selected experimental data

Reference	Material	Method	Measured temperature	Uncertainty
Kato *et al*. [Kat09]	0.12 ≤ y ≤ 0.60 O/M ≥ 1.922	Conventional thermal arrest technique Closed crucible	Solidus Liquidus	T ± 35 K
Böhler *et al*. [Boh14]	0.09 ≤ y ≤ 1 O/M ~ 2.00	Laser heating Under Ar (low Pu contents) and air (high Pu contents) Static atmosphere	Solidus Liquidus	T ± 60 K O/M ± 0.01
Fouquet-Métivier [Fou22] ESNII+ [Mar17,Sta17] ESFR-SMART [Mik17]	0.24 ≤ y ≤ 45 O/M = 1.98, 2.00	Laser heating Under Ar pO_2 measurement	Solidus	T ± 50 K O/M ± 0.01
Desagulier [Des23] PUMMA [Mar25]	0.60 ≤ y ≤ 0.70 O/M=1.99, 1.98	Laser heating Under Ar and Ar+H_2 (reducing atmosphere) pO_2 measurement	Solidus	T ± 50 K O/M ± 0.01
Martin *et al*. PUMMA [Mar25]	y=1, O/M~2, O/M<2	Laser heating Under flow of Ar and Ar+H_2 (reducing atmosphere) pO_2 measurement	Solidus	T ± 50 K O/M ± 0.01

This project has received funding from the Euratom research and training programme 2019-2020 under grant agreement No 945022.

Figure 2. Selected temperature data as a function of Pu content for O/M of 2.00 (a), 1.99 (b), 1.98 (c) and 1.97 (d) using the measurements in Table 1

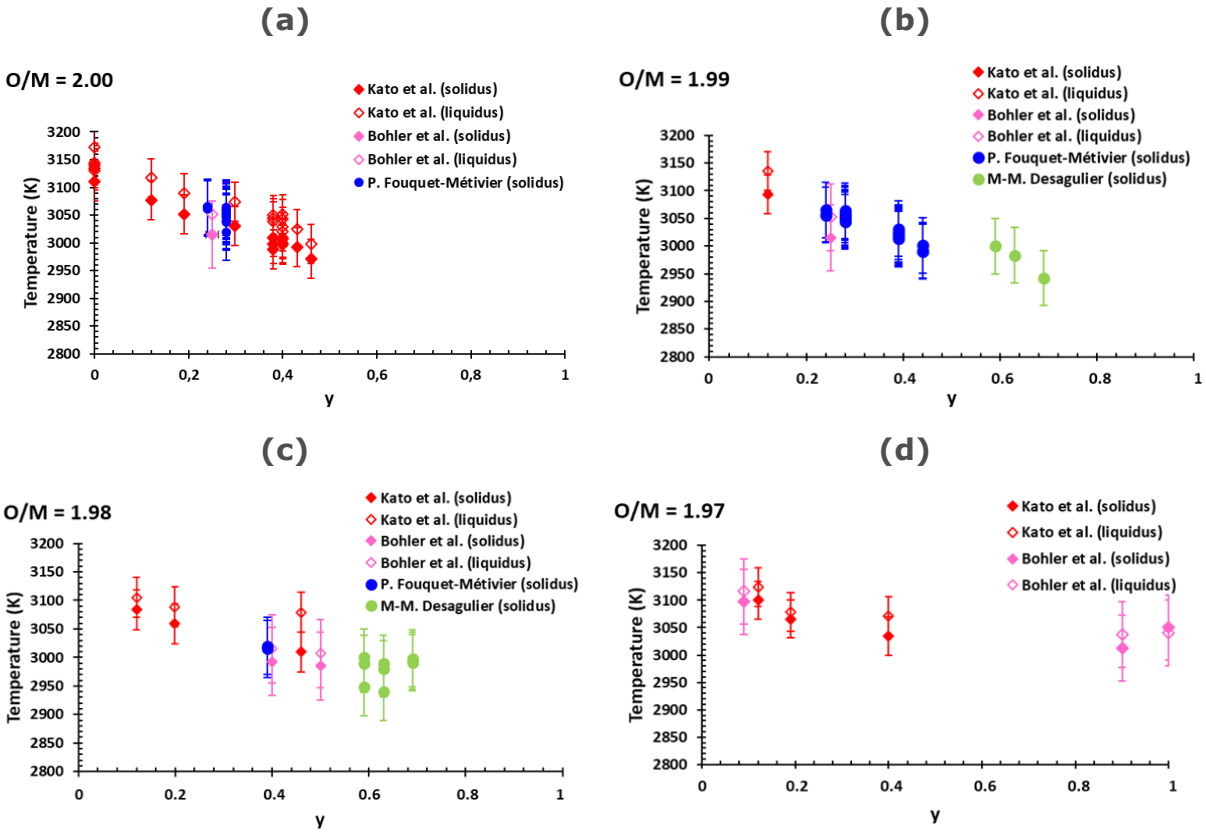

3. Models

Two types of models are presented in this section. Firstly, the thermodynamic modelling using the CALPHAD method [Fou23] is reported. Then a new correlation law is described using the selected data (section 2.4), to be used in the Fuel Performance Codes.

3.1 CALPHAD model

The principle of the CALPHAD method is to develop a thermodynamic database containing Gibbs energy functions for all solid, liquid and gas phases as a function of composition, temperature and pressure. At given conditions in temperature, composition and pressure, thermodynamic equilibrium can then be calculated by minimizing the total Gibbs energy of the system.

For the U-Pu-O system, models on the three U-O, Pu-O and Pu-U binary sub-systems were first built [Gue11]. For each binary system, the Gibbs energy functions are optimized to reproduce both phase diagram (phase boundaries) and thermodynamic data (enthalpy of formation, standard entropy, heat capacity, chemical potentials, mixing enthalpy ….). The advantage is that the derived model is consistent with both phase diagram and thermodynamic data.

This project has received funding from the Euratom research and training programme 2019-2020 under grant agreement No 945022.

Once the binary systems are assessed, it is possible to perform calculations on the ternary system by extrapolating from the binary sub-systems. However in most of the cases, it is necessary to add ternary interaction parameters to describe the ternary phase diagram and ternary phase properties.

The first version of the CALPHAD model on U-Pu-O was published by Guéneau *et a.l* in 2011 [Gue11]. Recently, the model for the liquid phase was improved by Fouquet-Métivier *et al*. [Fou23] to better describe solid/liquid transitions for $(U,Pu)O_{2\pm x}$ mixed oxides, based on the selected data of Kato [Kat09] and Bohler *et al.* [Boh14]. This model was introduced in version 18 of TAF-ID database [Gue21].

In the present work, we are comparing our results calculated with the CALPHAD model of Fouquet-Métivier *et a.l* [Fou23] with all the available experimental data selected in section 2.4. The results are presented in Appendix 6.1.1 for fixed Pu contents and in Appendix 6.1.2 for fixed O/M ratios.

It has to be kept in mind that according to the CALPHAD model, based on oxygen potential data, both pure oxides have a congruent melting point for O/M slightly lower than 2: $UO_{1.98}$ and $PuO_{1.96}$. In U-O system, for lower and higher O/U ratio, the solidus and liquidus temperature decreases with the deviation from 1.98. In Pu-O system, the behaviour is different as only PuO_{2-x} exists. At high temperature, as its oxygen potential is higher than the one of UO_2, Pu dioxide has the tendency to lose oxygen and to be slightly reduced into PuO_{2-x} below its melting point. As a result, the oxygen release leads to the existence of phase equilibria between PuO_{2-x}, the gas phase and the liquid phase. The congruent melting point is found for $PuO_{1.96}$ (see Appendix 6.1.1 and 6.1.2).

In $(U,Pu)O_{2\pm x}$ mixed oxides, the exact composition and temperature of the congruent melting is not known. Only the experimental data of Kato [Kat09] measured for low O/M ratio show that the maximum is located for an O/M ratio below 1.94 for 20 Pu and below 1.9 for 40 Pu. The position of the maximum is shifted to lower O/M ratio when the Pu content increases, in agreement with the CALPHAD model. This has been explained by Fouquet-Métivier *et al.* [Fou23] by the stabilization of the mixed oxides in the region with O/M ratio below 2 due to the increase of the configurational entropy related to the formation of point defects (Pu^{3+} and oxygen vacancies).

The comparison of the calculated isopleth sections for fixed Pu contents (Appendix 6.1.1) with experimental data show:

- For 10 Pu: The CALPHAD model is in agreement with the lower values measured by Kato;
- For 20 Pu: The model tends to underestimate the solidus temperature compared to the data of Kato, especially for O/M ratio >1.95;
- For 25 Pu: The model is very good agreement with the data of Böhler *et al.*, not consistent with the recent data of Fouquet-Métivier which are very close to the liquidus temperature measured by Böhler;
- For 30 Pu-45 Pu: The model underestimates the solidus temperature compared to all the experimental data, especially for O/M>1.97;

This project has received funding from the Euratom research and training programme 2019-2020 under grant agreement No 945022.

- For 50-63 Pu: The agreement with the experimental data is reasonable when considering the scattering of the experimental data;

- For 69-100 Pu: The model tends to systematically underestimate the solidus temperature.

In the isopleth sections calculated for fixed O/M ratio (Appendix 6.1.2), the calculated results show this underestimation of the solidus temperature for O/M=2-1.99 whereas the agreement with the experimental data is reasonable for O/M=1.98-1.97. A break in the solidus curves is visible for O/M=2-1.98 for a Pu content close to y=0.5-0.7 that corresponds to the minimum temperature. This break is due to the formation of the gas phase in equilibrium with the solid and the liquid for higher Pu contents. This is related to the fact that the congruent melting point of PuO2 with our model is calculated for an O/M=1.95.

To conclude, the CALPHAD thermodynamic model, based on an extensive dataset of experimental thermodynamic and phase diagram data, shows the right shape of the solidus/liquidus surface in this complex $(U,Pu)O_{2\pm x}$ region. However it tends to systematically underestimate the solidus temperature, especially compared to the most recent measurements of Fouquet-Métivier [Fou22] and Desagulier [Des23] that were not taken into account in [Fou23]. This model will have therefore to be improved.

3.2 New MOX melting temperature correlation

Data considered in this work for the $(U,Pu)O_2$ fuel system are summarized in Table 1.

The mathematical formulation of the model for $(U,Pu)O_{2-x}$ is reported in Equation 1, which holds for fresh fuels.

$$T_{m,fresh} = T_{m,UO_2} + A_1 \cdot [Pu] + A_2 \cdot [Pu]^2 + B_1 \cdot |O/M - O/M_{max}| \quad [1]$$

where $T_{m,UO2}$ = 3132 K, based on data for UO_2 [Kat09], while [Pu] concentrations is a value between 0 and 1. The O/M_{max} (i.e., the O/M ratio corresponding to the maximum solidus temperature) is modelled as a function decreasing with Pu content up to [Pu] = 0.65 and, then increasing, i.e.:

$$O/M_{max} = \begin{cases} 2 - 0.3077 \cdot [Pu] \; if \; [Pu] < 0.65 \\ 1.8 + 1.5214 \cdot [Pu] \; if \; [Pu] > 0.65 \end{cases}$$

The calculated solidus surface is shown in Figure 3 as a function of Pu content and O/M ratio.

As an attempt, another additional term was considered in Eq. (1), namely a term

accounting for deviation from stoichiometry and plutonium content (B2· [Pu] · |O/M − O/Mmax|), but this was excluded because of its high p-value. This is a reasonable outcome, considering the spread of MOX melting data with O/M.

This project has received funding from the Euratom research and training programme 2019-2020 under grant agreement No 945022.

Values for the model regressors obtained via best fit of the data (Table 1), with associated standard errors and p-values, are reported in Table 2.

It can be seen that the statistical parameters for the trend of melting temperature with Pu content are better, as its behaviour is fairly well defined, with a minimum around 65% of Pu content. On the other hand, the regressor related to the behavior with stoichiometry variation has a larger standard error and a higher p-value, this is related to the scattering of the data.

Consequently, the coefficient of determination R2 turns out to be 0.69, an acceptable value, which, however, reflects the dispersion of the dataset.

The proposed correlation is evaluated against state-of-the-art correlations, i.e. the one from Magni et al. [Mag20] and Di Gennaro et al. [Dig25] that we assume to be our best-estimate reference correlation. Results obtained with Calphad calculations [Fou23] are also reported as a benchmark. A comparison for O/M = 2 considering the whole Pu domain is shown in Figure 4, while the behaviour of the new correlation is shown for several fixed values of plutonium content in the whole O/M domain in Figure 5 and for several fixed values of O/M in the whole Pu domain in Figure 6. Residuals are shown in Figure 7 and Figure 8, highlighting the good performance of the proposed correlation, with most of the data (around 90%) lying within the 1% deviation band (corresponding to the best experimental uncertainty currently associated to melting temperature measurements).

The model proposed captures this non-ideal behaviour of mixed-oxide fuels (while O/Mmax= 2.00 for UO2 – ideal behaviour), as well as the behaviour of the property at high Pu contents, such as the latest experimental data from this project at Pu contents between 60 and 80%. The calculated Mean absolute Error (MAE) of the model is equal to 15.76 K, and the Mean Absolute Percentage Error (MAPE) is equal to 0.5 %. In the appendix (6), results shown in Figure 5 and Figure 6 are expanded, showing the comparison with state-of-the-art correlation for all the selected values of O/M (6.2.1) and plutonium content (6.2.2).

Table 2 : Results from the best fit of the model for the solidus temperature of $(U,Pu,)O_{2\pm x}$.

Regressor	Units	Estimate	Std. Error	p-value
A_1	K	-299.58	38.70	$< 10^{-10}$
A_2	K	210.46	34.63	$< 10^{-7}$
B_1	K	-251.78	88.4	$< 10^{-3}$

This project has received funding from the Euratom research and training programme 2019-2020 under grant agreement No 945022.

Figure 3 : Solidus temperature of MOX fuels as a function of the Pu content and the O/M ratio against experimental data from Table 1. The congruent melting line is highlighted in black.

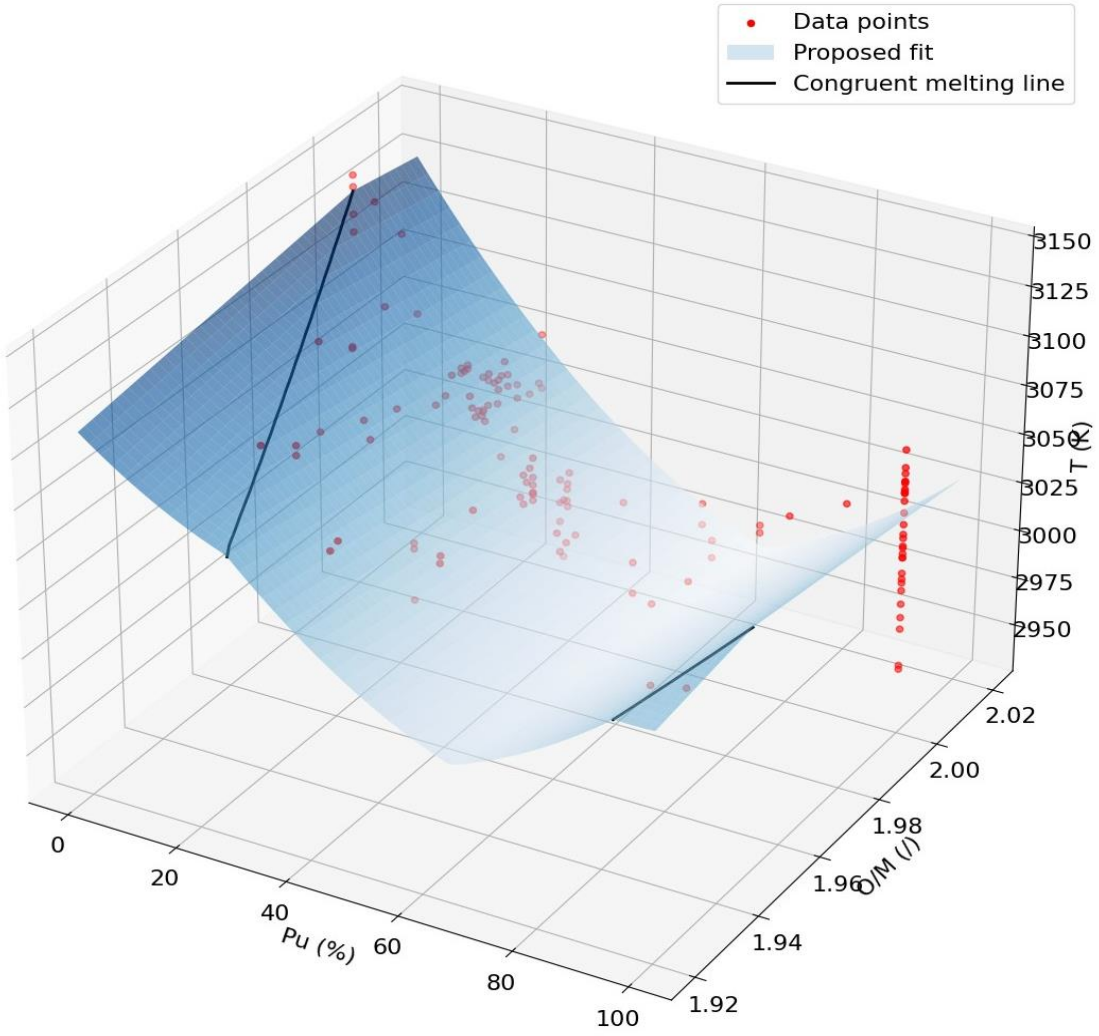

This project has received funding from the Euratom research and training programme 2019-2020 under grant agreement No 945022.

Figure 4 : Solidus temperature of MOX fuels as a function of the Pu content: behaviour of the novel model (black line), compared to the state-of-the-art models (blue dashed line, extrapolated out-of-range of validity for [Pu] > 45%).

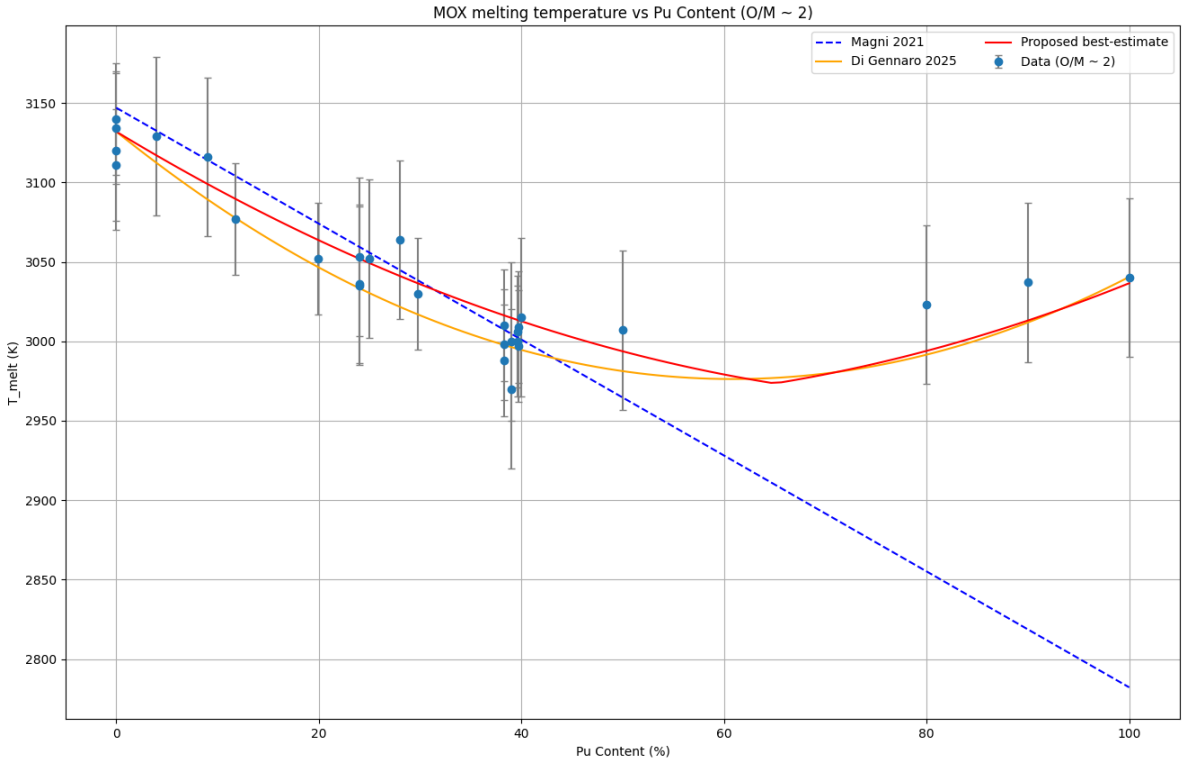

Figure 5 : Solidus temperature of MOX fuels as a function of the O/M ratio for various Pu contents (0% - 20% - 40% - 60% - 80% - 100%) compared to experimental data for each selected Pu content.

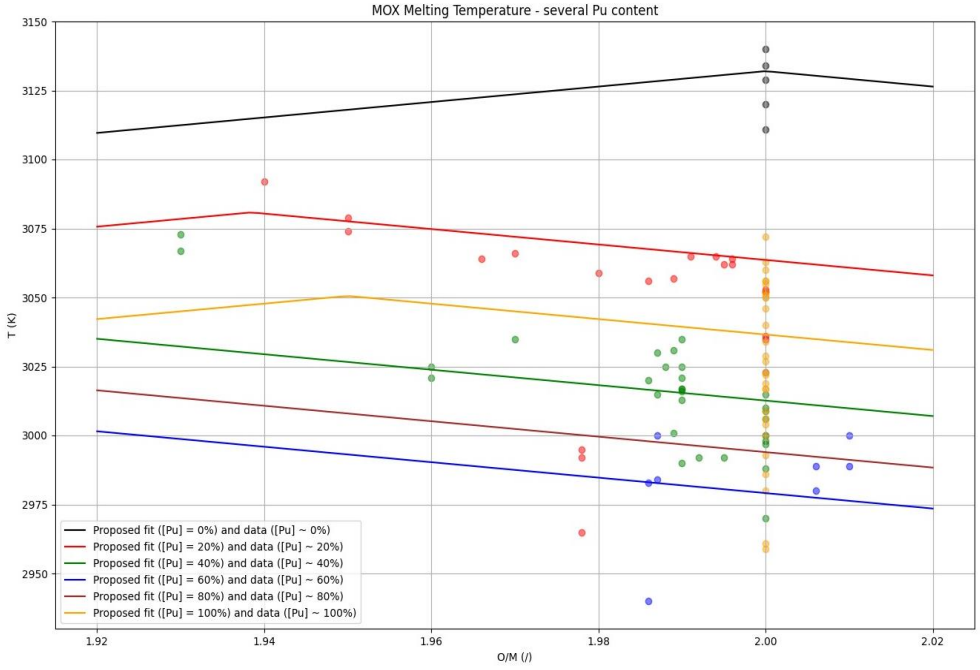

This project has received funding from the Euratom research and training programme 2019-2020 under grant agreement No 945022.

Figure 6 : Solidus temperature of MOX fuels as a function of the Pu content for various O/M ratios (2 - 1.99 - 1.98 - 1.97) compared to experimental data for each selected O/M.

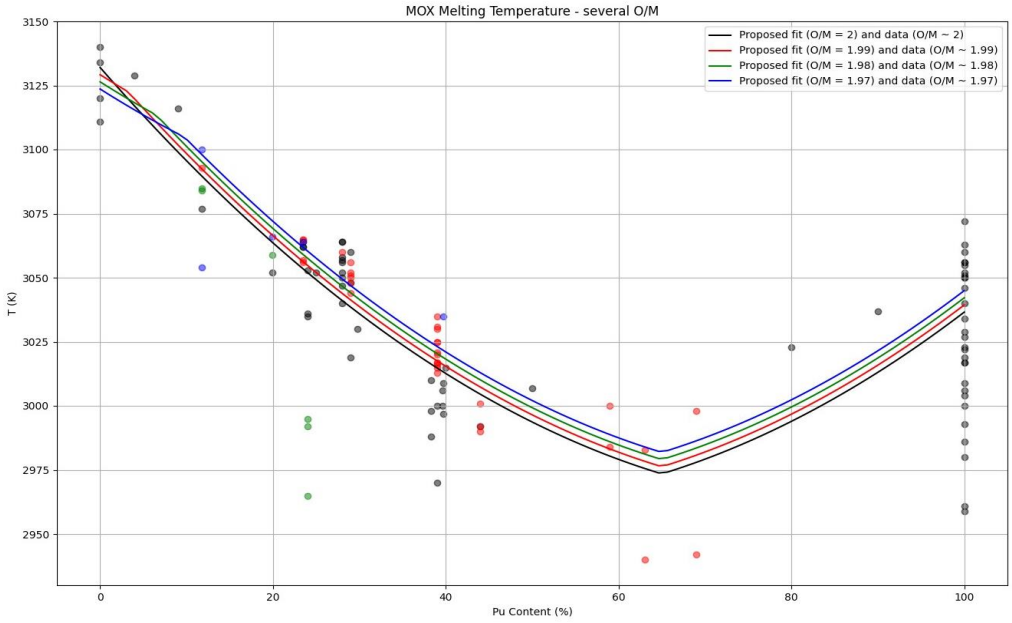

Figure 7 : Comparison between calculated and measured solidus temperatures of $(U,Pu)O_{2-x}$ fuels.

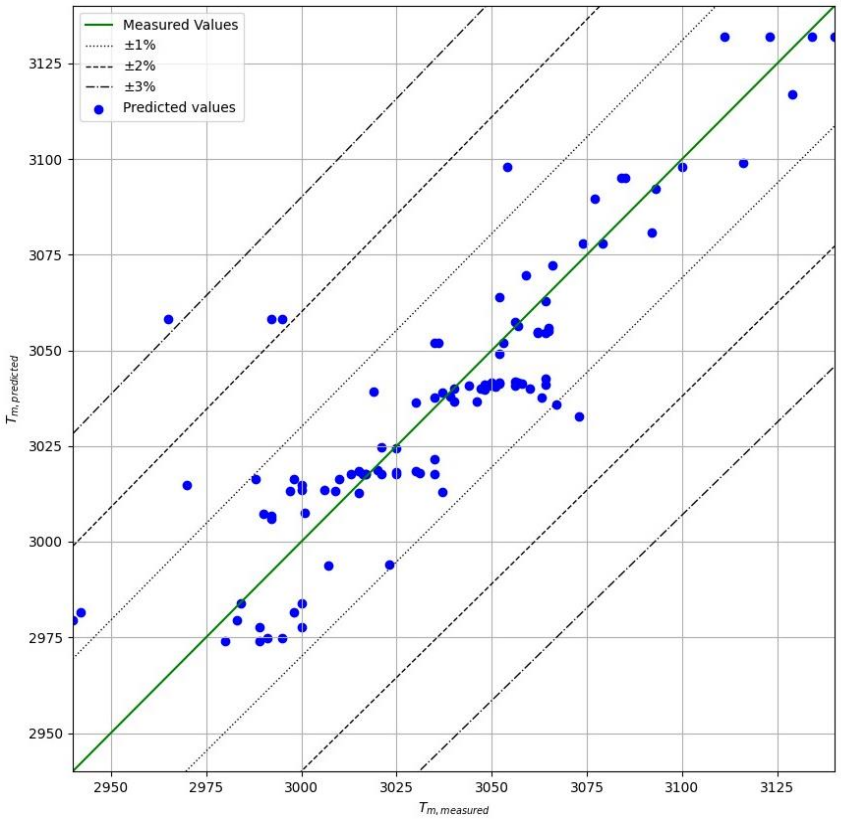

This project has received funding from the Euratom research and training programme 2019-2020 under grant agreement No 945022.

Figure 8 : Comparison between residuals against Pu content for the novel correlation with respect to state-of-the-art models.

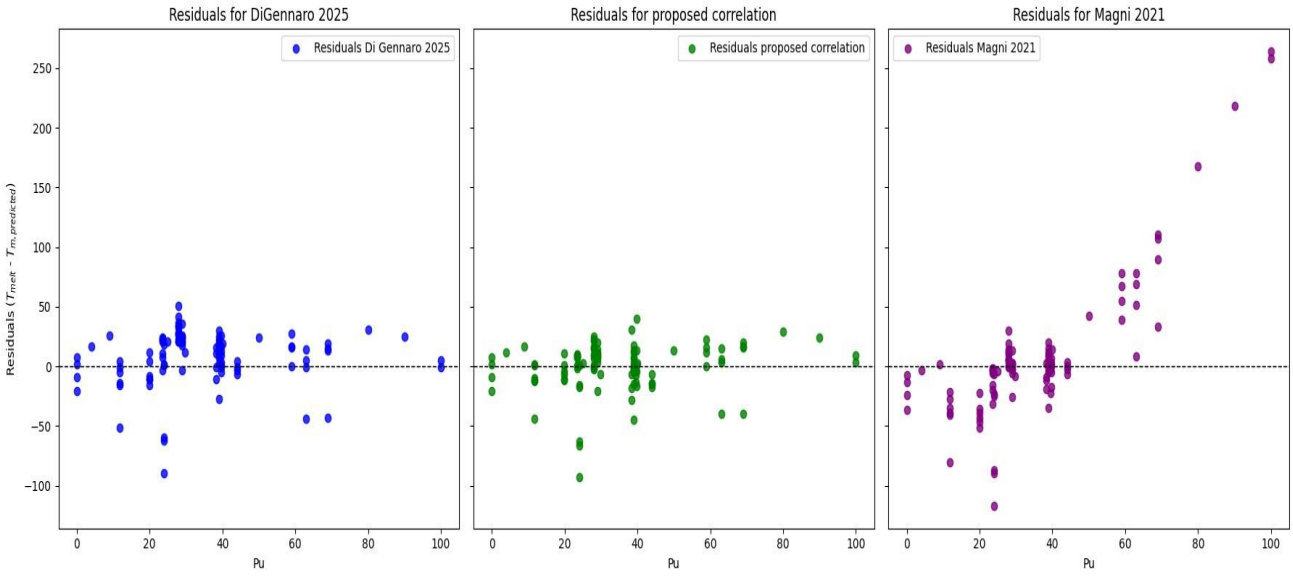

4. Conclusion

In this work, all available data on the melting temperature of (U,Pu)$O_{2\pm x}$ fuel, measured using conventional thermal analysis at JAEA or an advanced laser heating technique at JRC, were reviewed. A selection of experimental data was proposed, based on uncertainty analysis on the O/M ratio and temperature.

Data calculated using the latest CALPHAD model, derived by Fouquet-Métivier *et al.*, were compared with these selected data. It was found that the model is in good agreement with experimental data for O/M ≤1.98 and tends to underestimate the solidus temperature of (U,Pu)$O_{2\pm x}$ fuel for O/M=1.99-2.0. The model therefore needs to be improved.

The selected experimental data were used to derive a new correlation law for fresh MOX fuels. The proposed correlation is in very good agreement with most of the data (around 90% lying within the 1% deviation band). Its good performance is promising for use in Fuel performance Codes.

In the future, simulations of thermograms and associated solidification phenomena occurring during cooling would be very useful for a better understanding of melting/solidification processes, and would help to reduce the remaining uncertainties, particularly on the O/M ratio of samples at the measured temperature. Additional melting temperature measurements for lower O/M ratios (below 1.92) would enable a wider range of O/M ratios to be covered, and the exact congruent melting temperature for MOX fuels to be determined.

5. References

[Boh14] R. Böhler *et al.*, 'Recent advances in the study of the UO2–PuO2 phase diagram at high temperatures', *Journal of Nuclear Materials*, vol. 448, no. 1–3, pp. 330–339, May 2014, doi: 10.1016/j.jnucmat.2014.02.029.

This project has received funding from the Euratom research and training programme 2019-2020 under grant agreement No 945022.

[Cas24] L. Casini *et al.*, 'Melting behavior of mixed plutonium and iron oxides: an experimental study', *Nuclear Materials and Energy*, Vol. 41, Dec. 2024, 101761, doi: 10.1016/j.nme.2024.101761

[Deb10] F. De Bruycker, K. Boboridis, D. Manara, P. Pöml, M. Rini, and R. J. M. Konings, 'Reassessing the melting temperature of PuO2', *Materials Today*, vol. 13, no. 11, pp. 52–55, Nov. 2010, doi: 10.1016/S1369-7021(10)70204-2.

[Deb11A] F. De Bruycker, K. Boboridis, P. Pöml, R. Eloirdi, R. J. M. Konings, and D. Manara, 'The melting behaviour of plutonium dioxide: A laser-heating study', *Journal of Nuclear Materials*, vol. 416, no. 1, pp. 166–172, Sep. 2011, doi: 10.1016/j.jnucmat.2010.11.030.

[Deb11B] F. De Bruycker *et al.*, 'On the melting behaviour of uranium/plutonium mixed dioxides with high-Pu content: A laser heating study', *Journal of Nuclear Materials*, vol. 419, no. 1, pp. 186–193, Dec. 2011, doi: 10.1016/j.jnucmat.2011.08.028.

[Des23] M.-M. Desagulier, 'Elaboration d'oxydes mixtes (U,Pu)O2-x à forte teneur en plutonium et mesure de leurs propriétés thermodynamiques et structurales', Thèse Université Montpellier, 2023.

[Dig25] M. D. Gennaro, A. Magni, M. Guarnieri, D. Pizzocri, L. Luzzi, C. Guéneau, P. V. Uffelen, Modelling and assessment of thermophysical properties of am-bearing fuels for transmutation purposes in fast reactors, Submitted to Progress in Nuclear Energy (2015).

[Fou22] P. Fouquet-Métivier, 'Study of the influence of americium on thermodynamic and structural properties of (U,Pu)O2x mixed oxides', Thèse Université Paris Saclay, 2022.

[Fou23] P. Fouquet-Métivier *et al.*, 'Investigation of the solid/liquid phase transitions in the U–Pu–O system', *Calphad*, vol. 80, p. 102523, Mar. 2023, doi: 10.1016/j.calphad.2022.102523.

[Kat08] M. Kato, K. Morimoto, H. Sugata, K. Konashi, M. Kashimura, and T. Abe, 'Solidus and liquidus of plutonium and uranium mixed oxide', *Journal of Alloys and Compounds*, vol. 452, no. 1, pp. 48–53, Mar. 2008, doi: 10.1016/j.jallcom.2007.01.183.

[Kat09] M. Kato, 'Melting temperatures of oxide fuel for fast reactors', presented at the ICAPP2009: 2009 international congress on advances in nuclear power plants, Tokyo, May 2009

[Gue11] C. Guéneau, N. Dupin, B. Sundman, C. Martial, J. C. Dumas, S. Gossé, S. Chatain, F. D. Bruycker, D. Manara, R. J. Konings, Thermodynamic modelling of advanced oxide and carbide nuclear fuels: Description of the U–Pu–O–C systems, Journal of Nuclear Materials 419 (2011) 145–167. doi:10.1016/J.JNUCMAT.2011.07.033.

[Gue21] C. Guéneau et al, TAF-ID: An international thermodynamic database for nuclear fuels applications, Calphad 72 (2021) 102212. doi: 10.1016/j.calphad.2020.102212

This project has received funding from the Euratom research and training programme 2019-2020 under grant agreement No 945022.

[Mag20] A. Magni, T. Barani, A. Del Nevo, D. Pizzocri, D. Staicu, P. Van Uffelen, L. Luzzi, Modelling and assessment of thermal conductivity and melting behaviour of mox fuel for fast reactor applications, Journal of Nuclear Materials 541, cited by: 21; All Open Access, Green Open Access, Hybrid Gold Open Access (2020). doi:10.1016/j.jnucmat.2020.152410.

[Man05] D. Manara, C. Ronchi, M. Sheindlin, M. Lewis, and M. Brykin, 'Melting of stoichiometric and hyperstoichiometric uranium dioxide', *Journal of Nuclear Materials*, vol. 342, no. 1, pp. 148–163, Jun. 2005, doi: 10.1016/j.jnucmat.2005.04.002.

[Man08] D. Manara, M. Sheindlin, W. Heinz, and C. Ronchi, 'New techniques for high-temperature melting measurements in volatile refractory materials via laser surface heating', *Review of Scientific Instruments*, vol. 79, no. 11, p. 113901, Nov. 2008, doi: 10.1063/1.3005994.

[Mar17] P. Martin et al, 'Catalog on MOX properties for fast reactors', ESNII+ project, Deliverable D7.5.1 (09/10/2017)

[Mar25] P. Martin et al, 'Results of measurements on fresh fuel', PUMMA project, Deliverable D3.7 (03/2025)

[Mik17] K. Mikityuk et al, 'New measurements of properties of MOX fuel with associated characterisations', ESFR-SMART project, Deliverable D10.5 (26/06/2023)

[Mor05] K. Morimoto *et al.*, 'Preparation and characterization of (Pu, U, Np, Am, simulated FP) O2−X', *Journal of Physics and Chemistry of Solids*, vol. 66, no. 2–4, pp. 634–638, Feb. 2005, doi: 10.1016/j.jpcs.2004.06.071.

[Sta17] D. Staicu et al, 'Measurement of properties of fresh PHENIX fuel', ESNII+ project, Deliverable D7.41 (29/09/2017)

[Str16] M. Strach, D. Manara, R. C. Belin, and J. Rogez, 'Melting behavior of mixed U–Pu oxides under oxidizing conditions', *Nuclear Instruments and Methods in Physics Research Section B: Beam Interactions with Materials and Atoms*, vol. 374, pp. 125–128, May 2016, doi: 10.1016/j.nimb.2016.01.032.

This project has received funding from the Euratom research and training programme 2019-2020 under grant agreement No 945022.

6. Appendix

6.1 Appendix 1: CALPHAD calculations

6.1.1 For fixed Pu contents

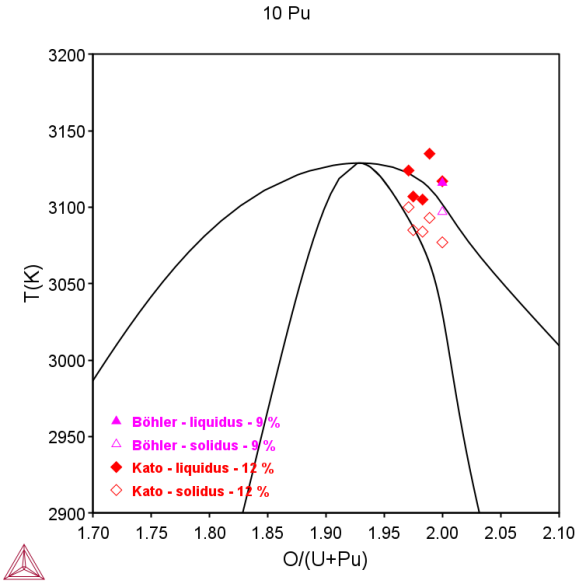

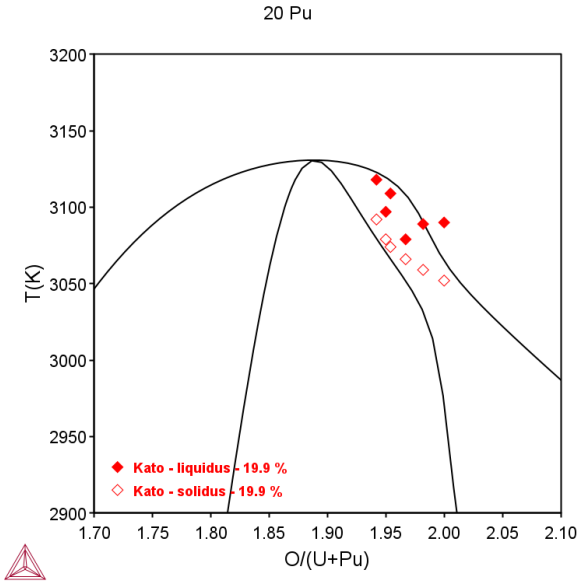

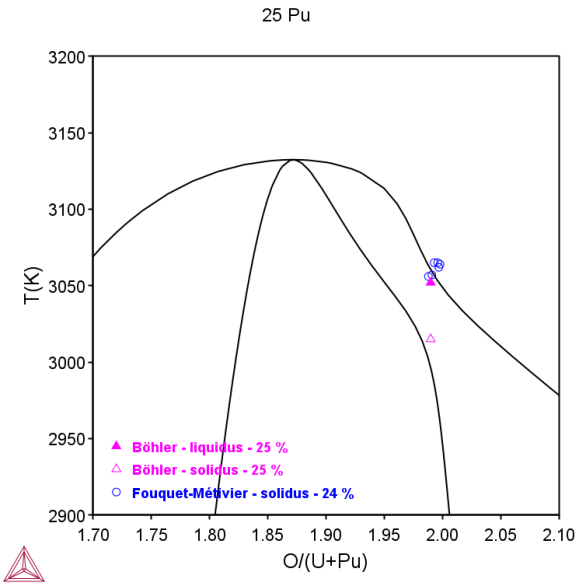

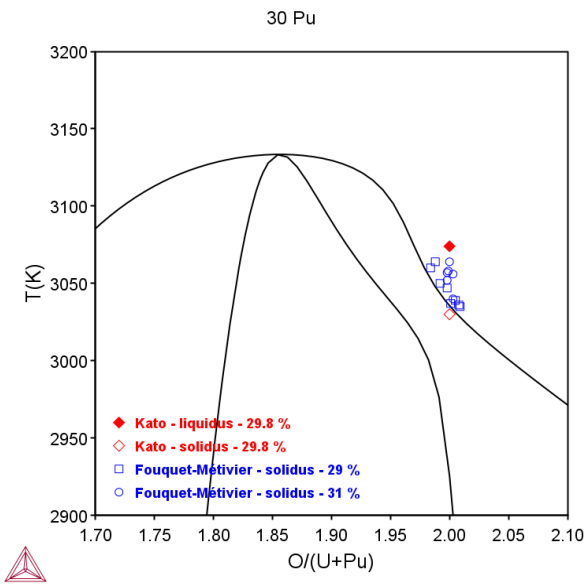

This project has received funding from the Euratom research and training programme 2019-2020 under grant agreement No 945022.

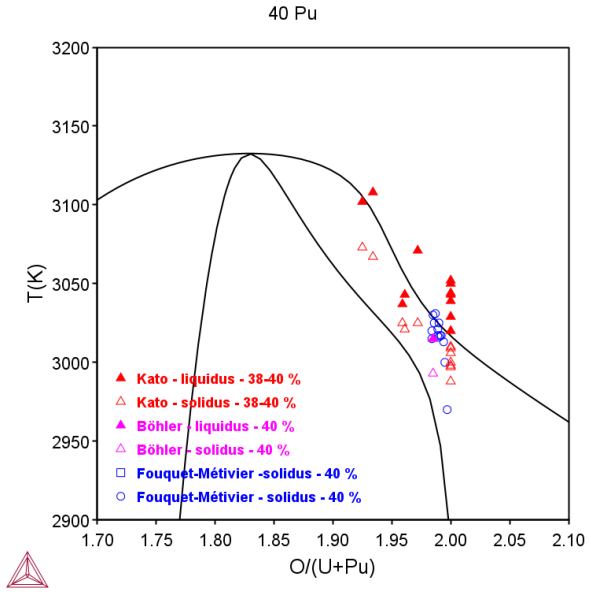

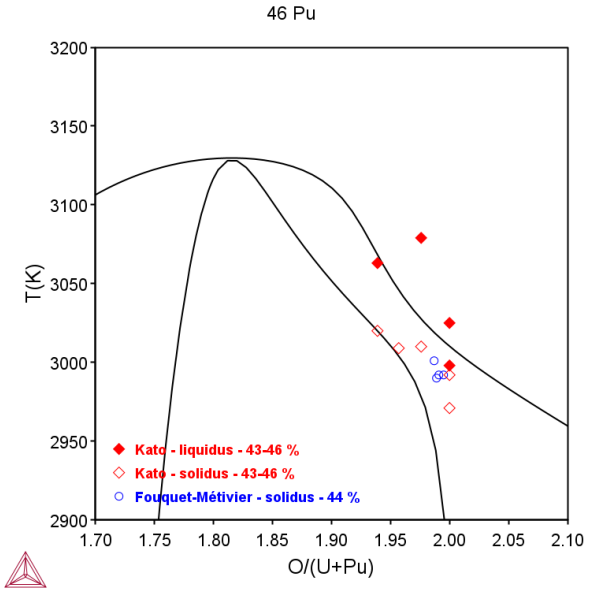

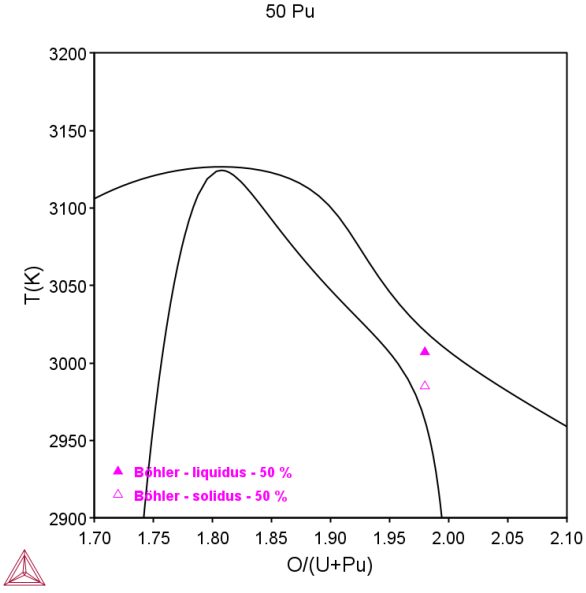

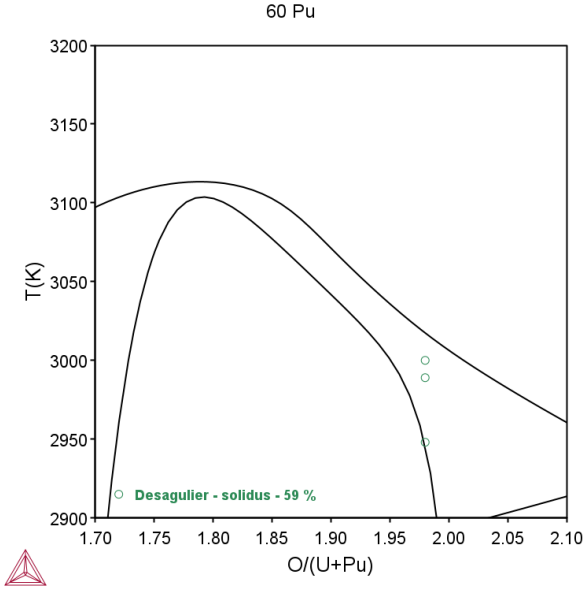

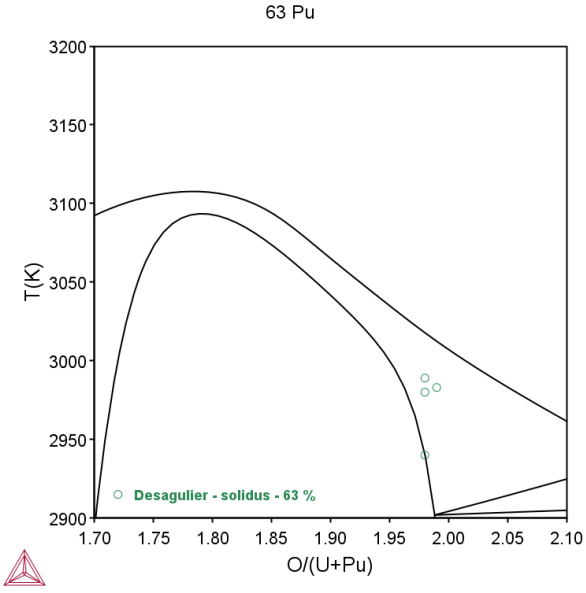

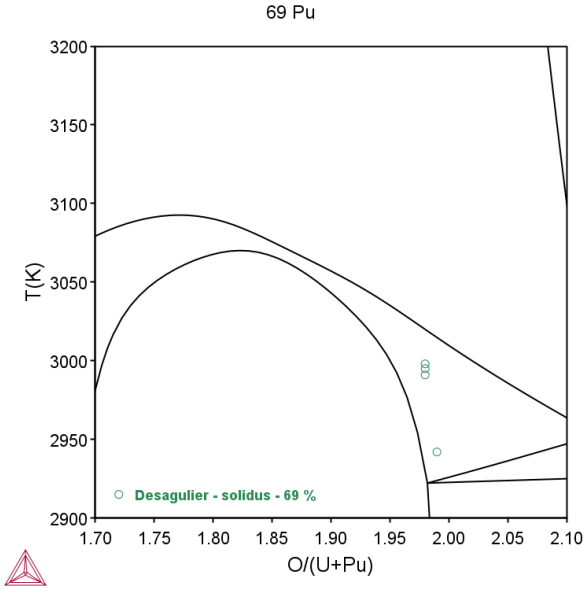

This project has received funding from the Euratom research and training programme 2019-2020 under grant agreement No 945022.

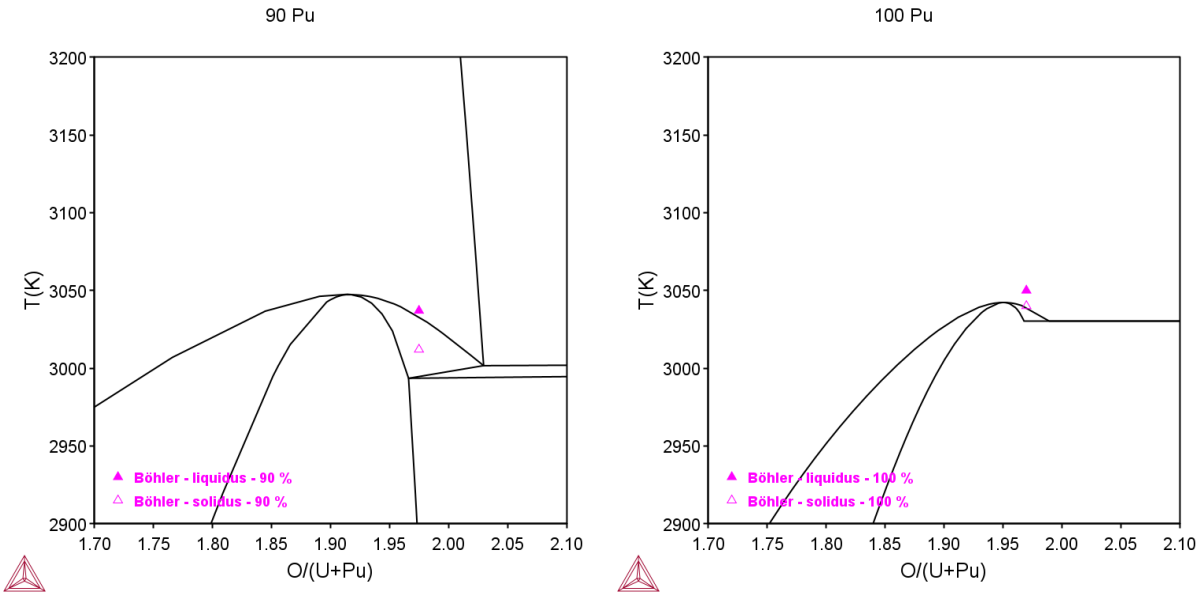

This project has received funding from the Euratom research and training programme 2019-2020 under grant agreement No 945022.

6.1.2 For fixed O/M ratio

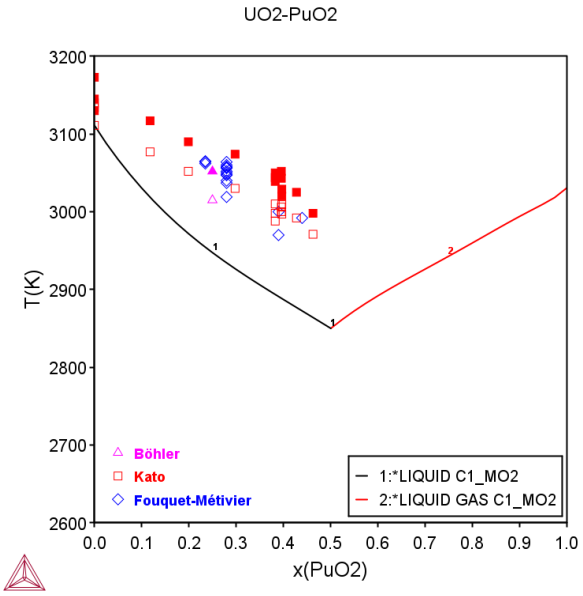

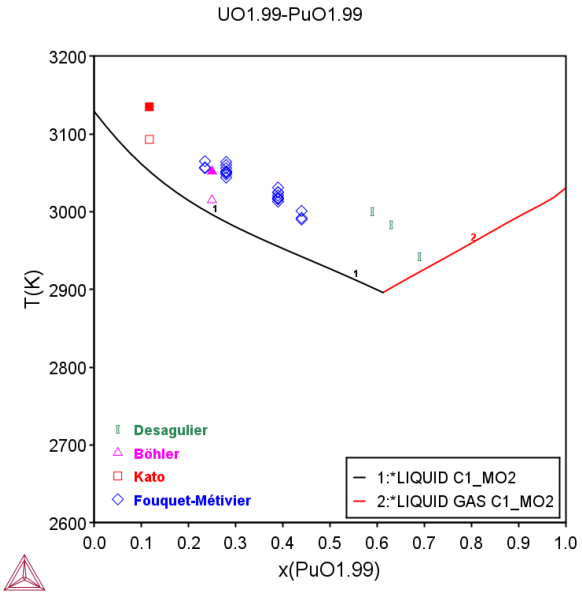

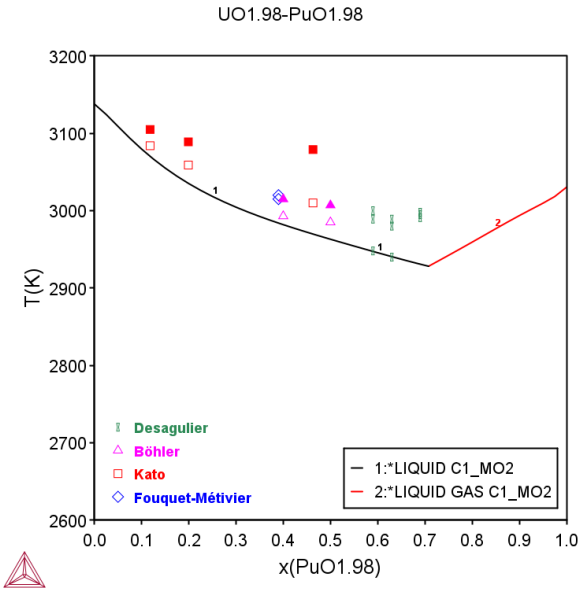

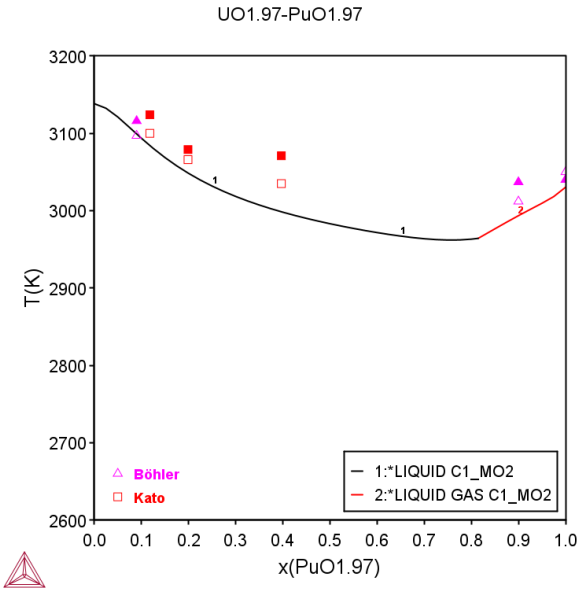

This project has received funding from the Euratom research and training programme 2019-2020 under grant agreement No 945022.

6.2 Appendix 2: Comparison between CALPHAD/correlations laws/exp. data

6.2.1 For fixed Pu contents

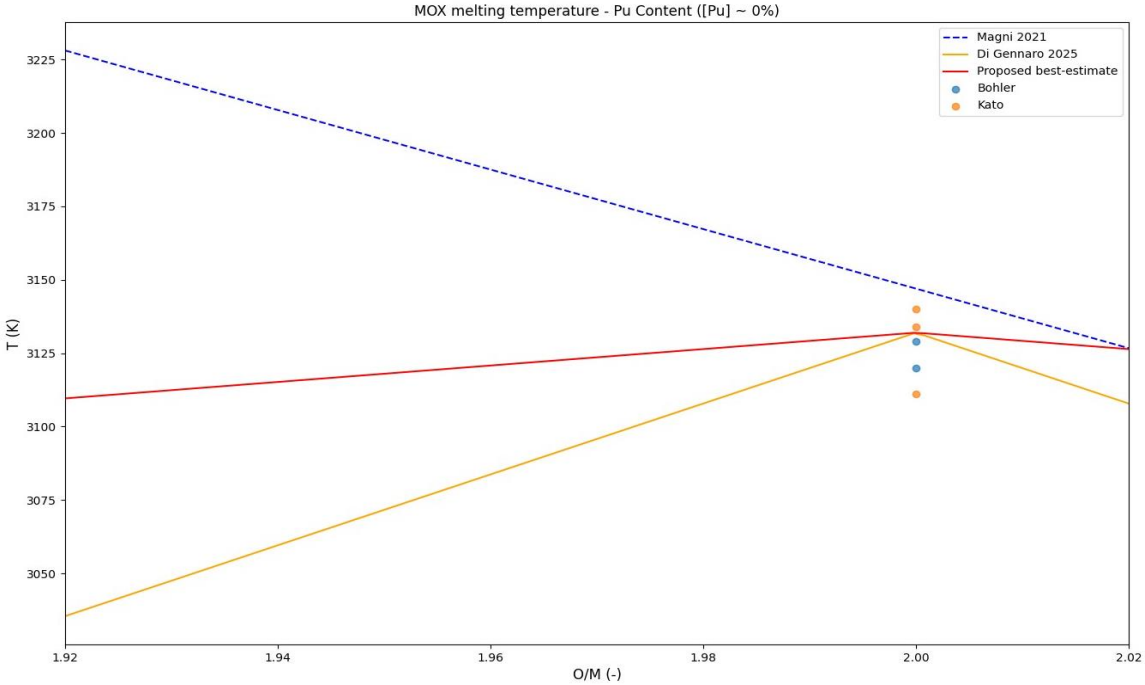

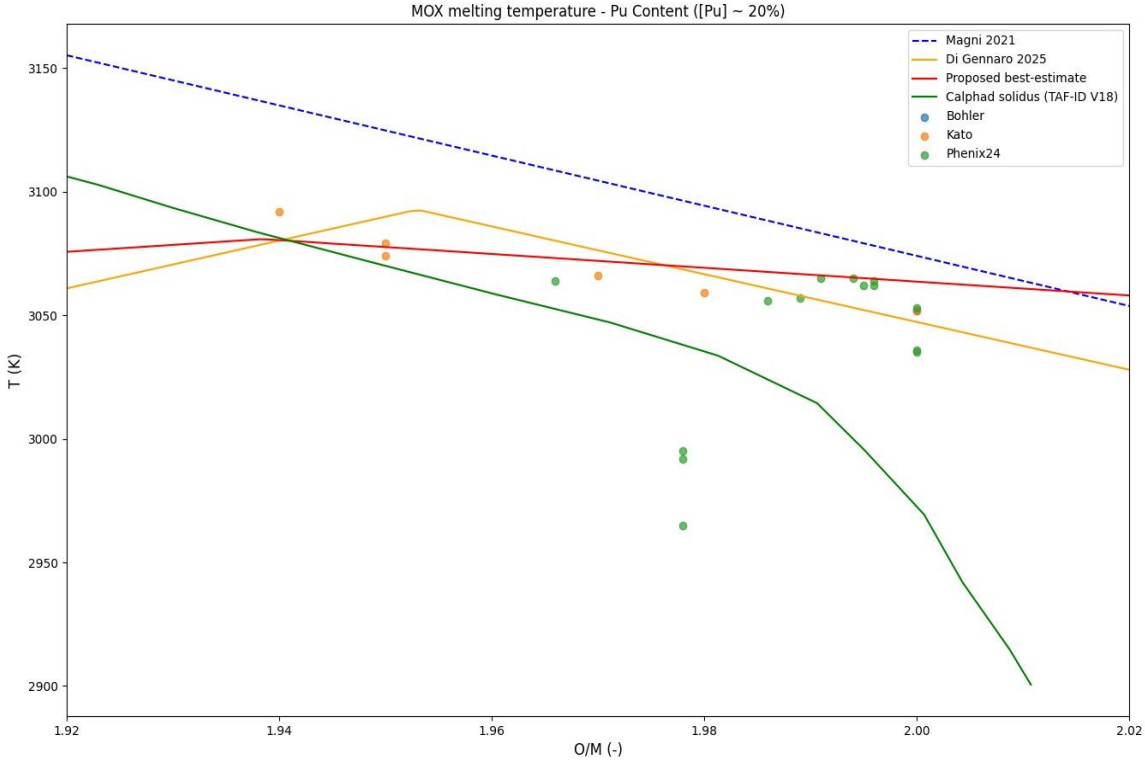

This project has received funding from the Euratom research and training programme 2019-2020 under grant agreement No 945022.

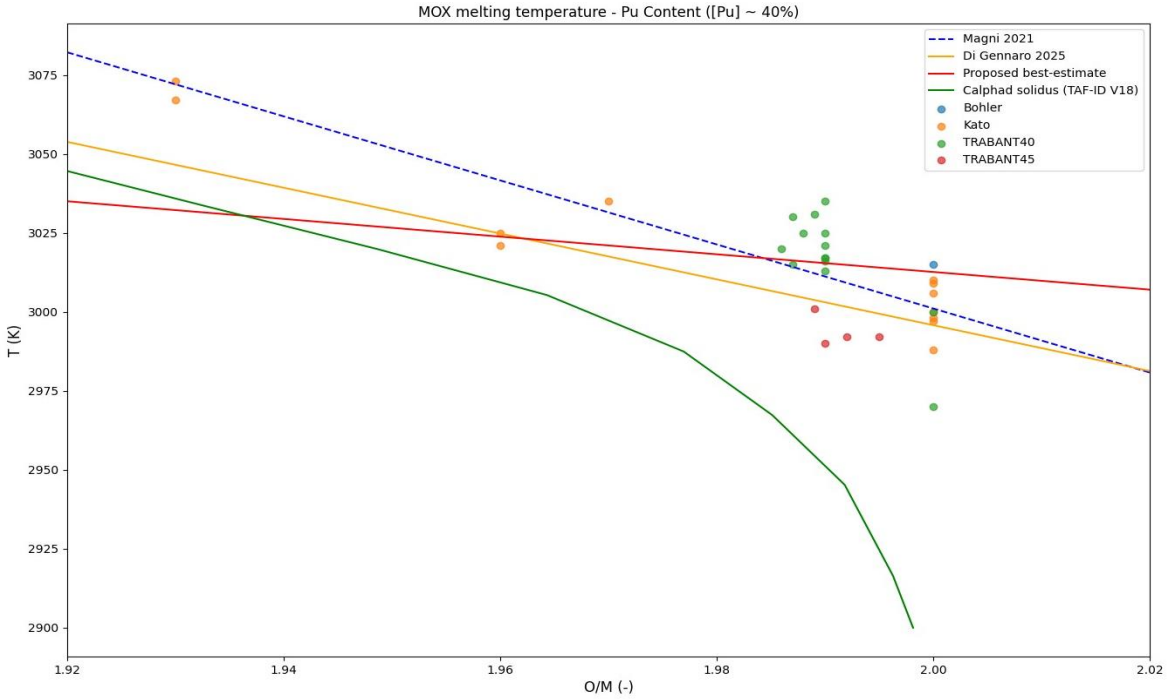

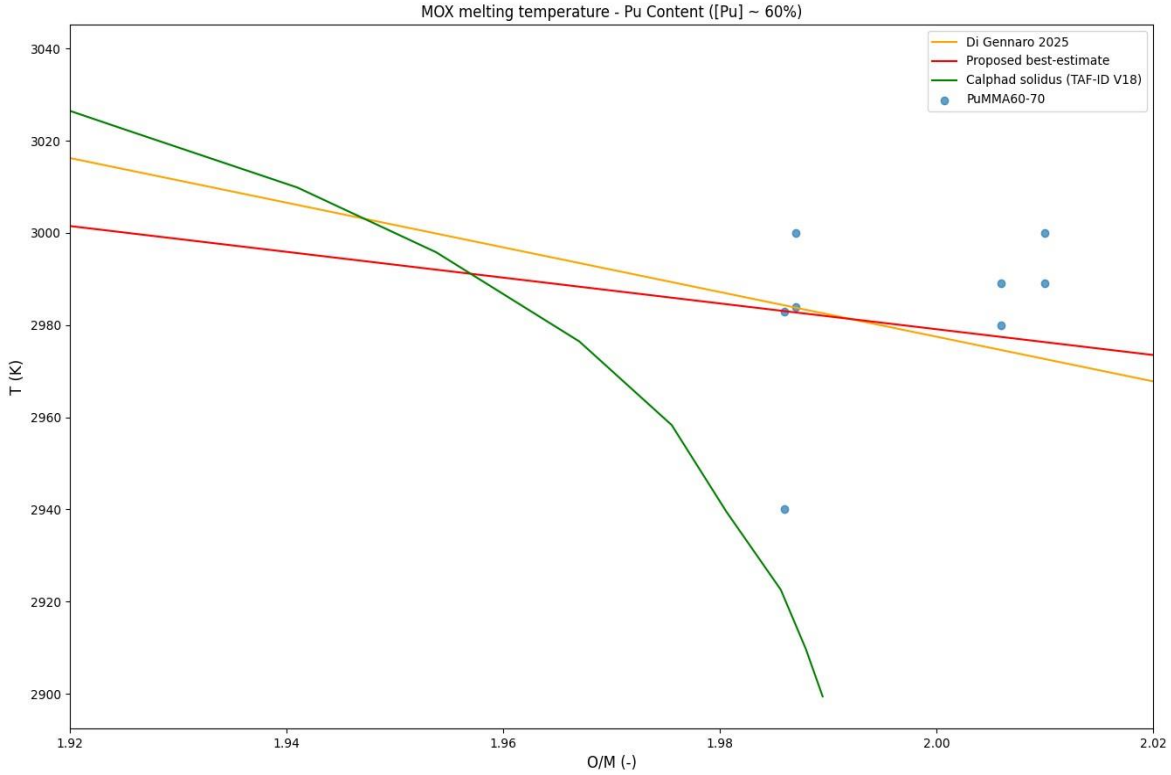

This project has received funding from the Euratom research and training programme 2019-2020 under grant agreement No 945022.

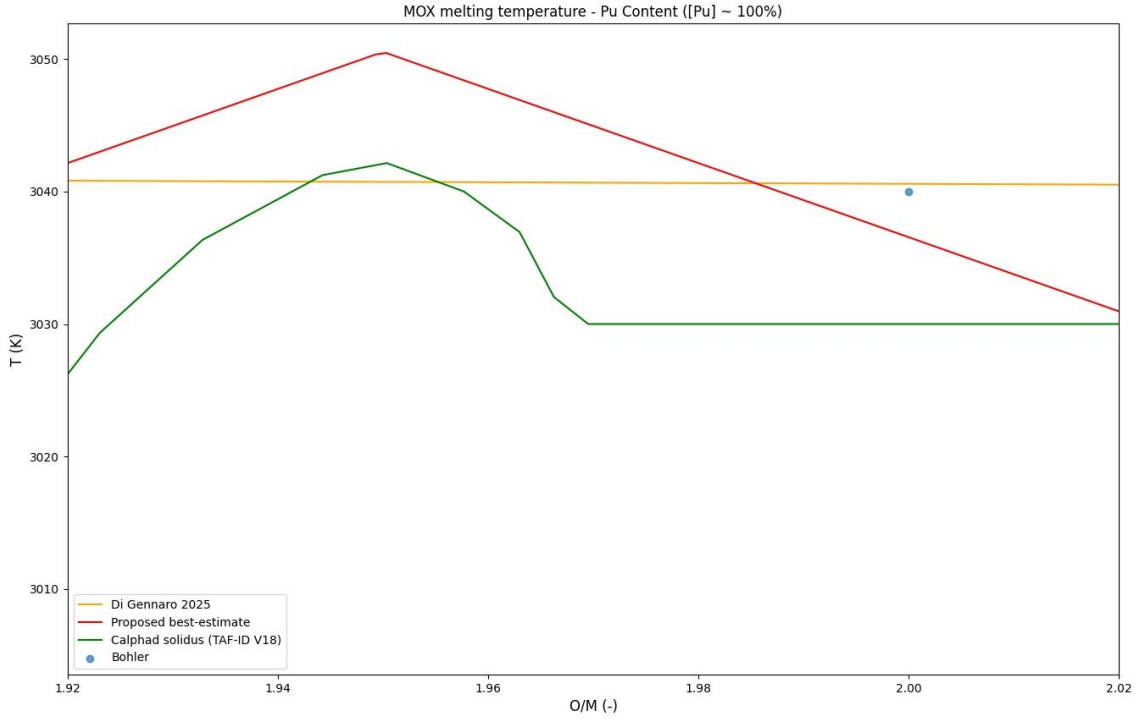

6.2.2 For fixed O/M ratio

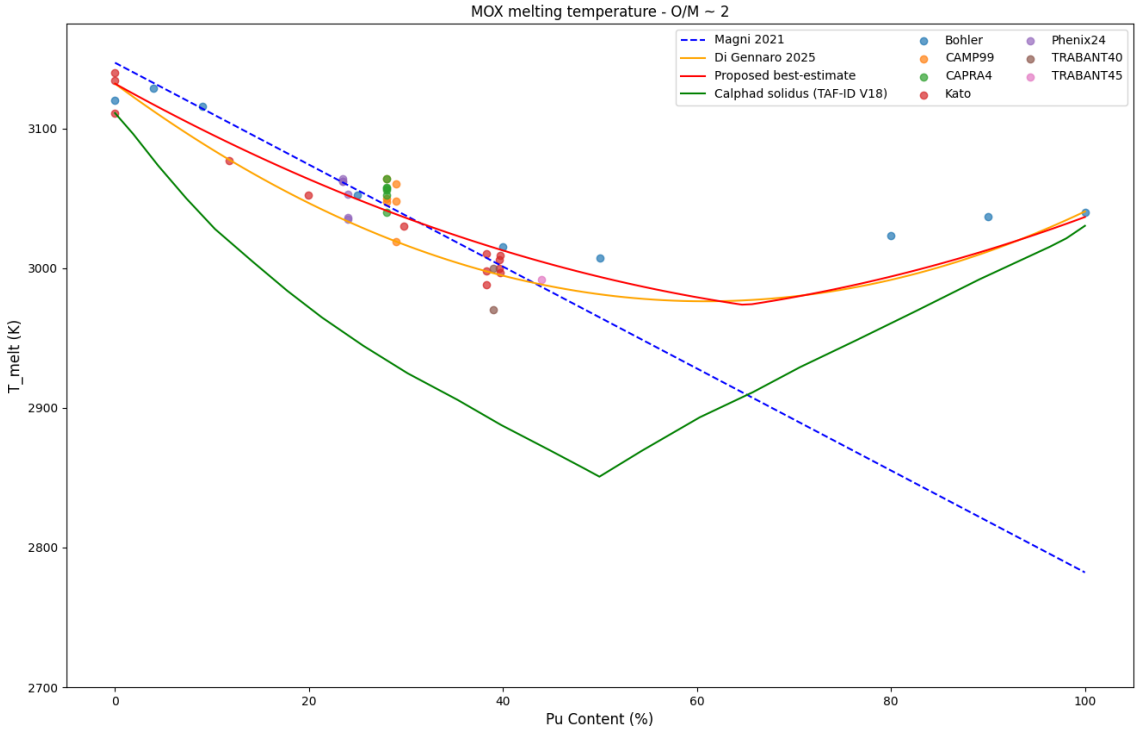

This project has received funding from the Euratom research and training programme 2019-2020 under grant agreement No 945022.

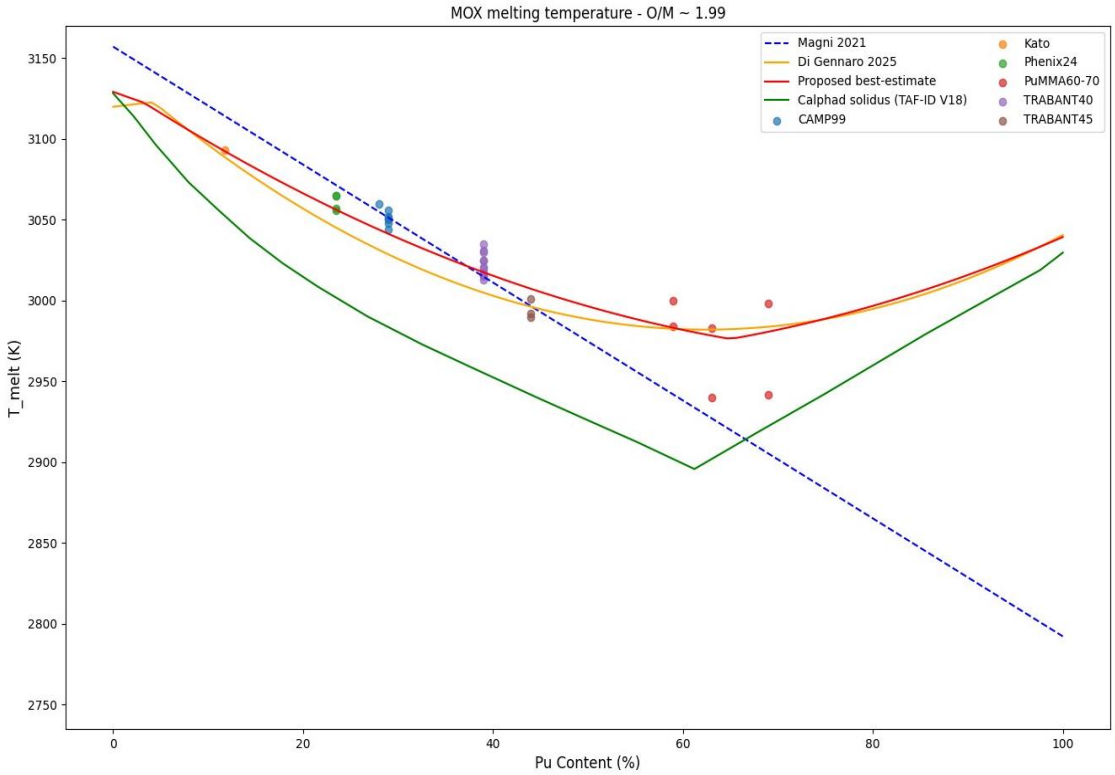

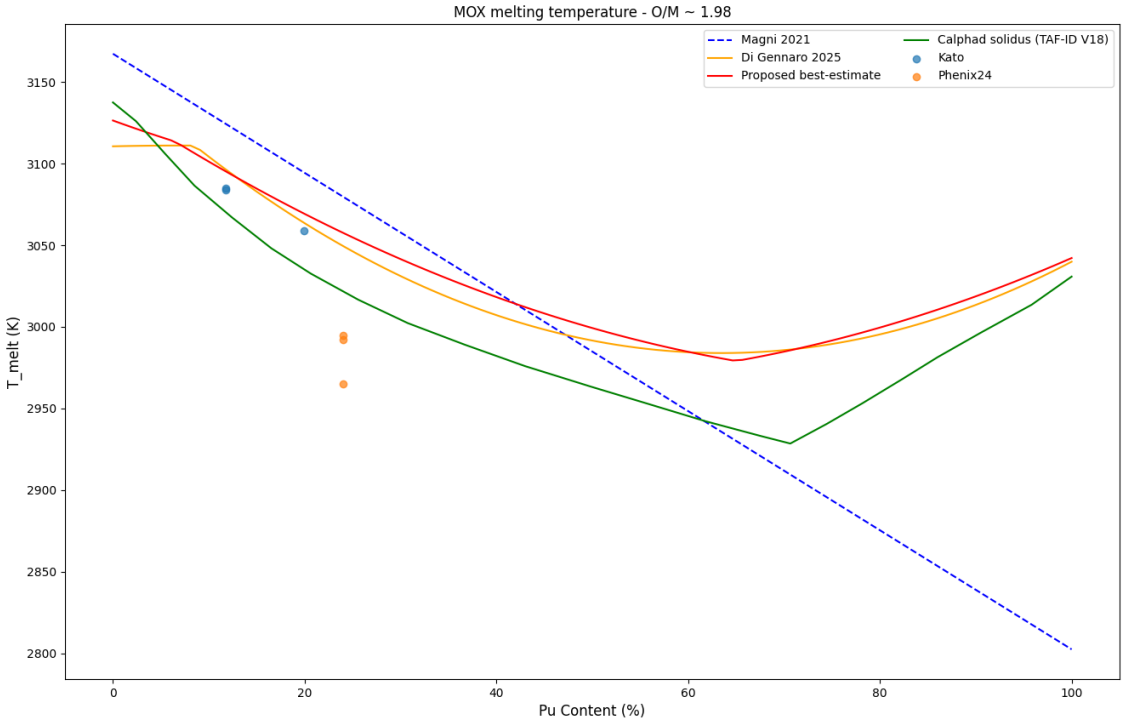

This project has received funding from the Euratom research and training programme 2019-2020 under grant agreement No 945022.

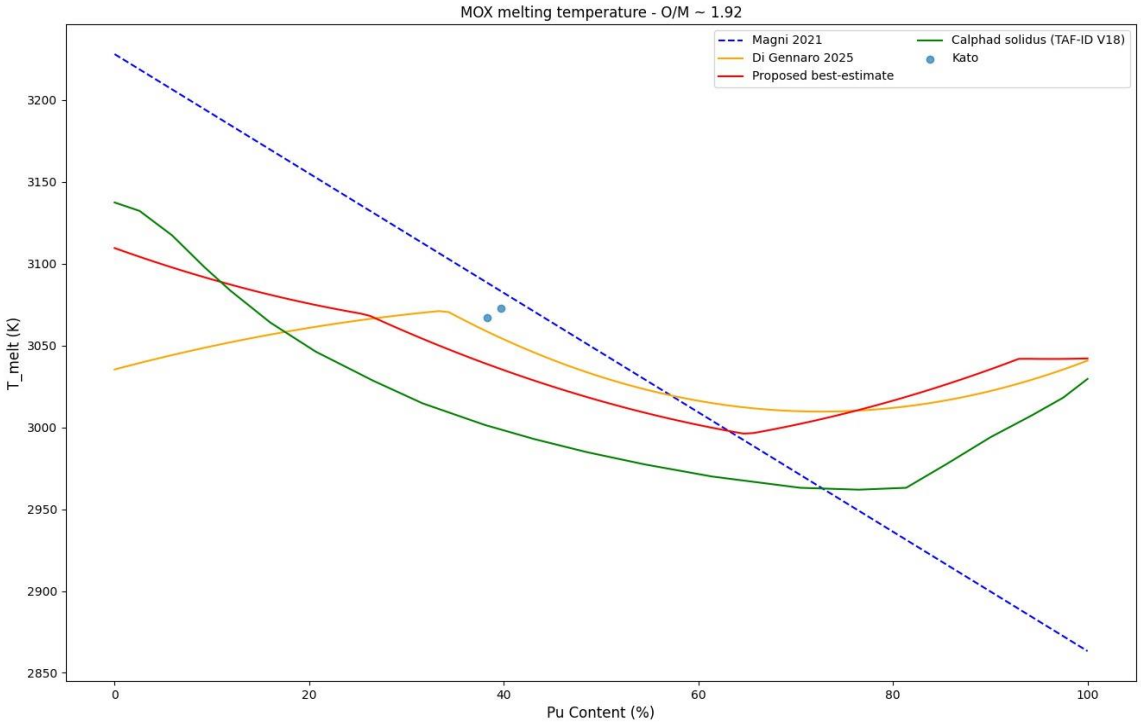

This project has received funding from the Euratom research and training programme 2019-2020 under grant agreement No 945022.

6.2.3 Comparison between calculated and measured solidus temperatures of $(U,Pu)O_{2-x}$ fuels, divided into subgroups.

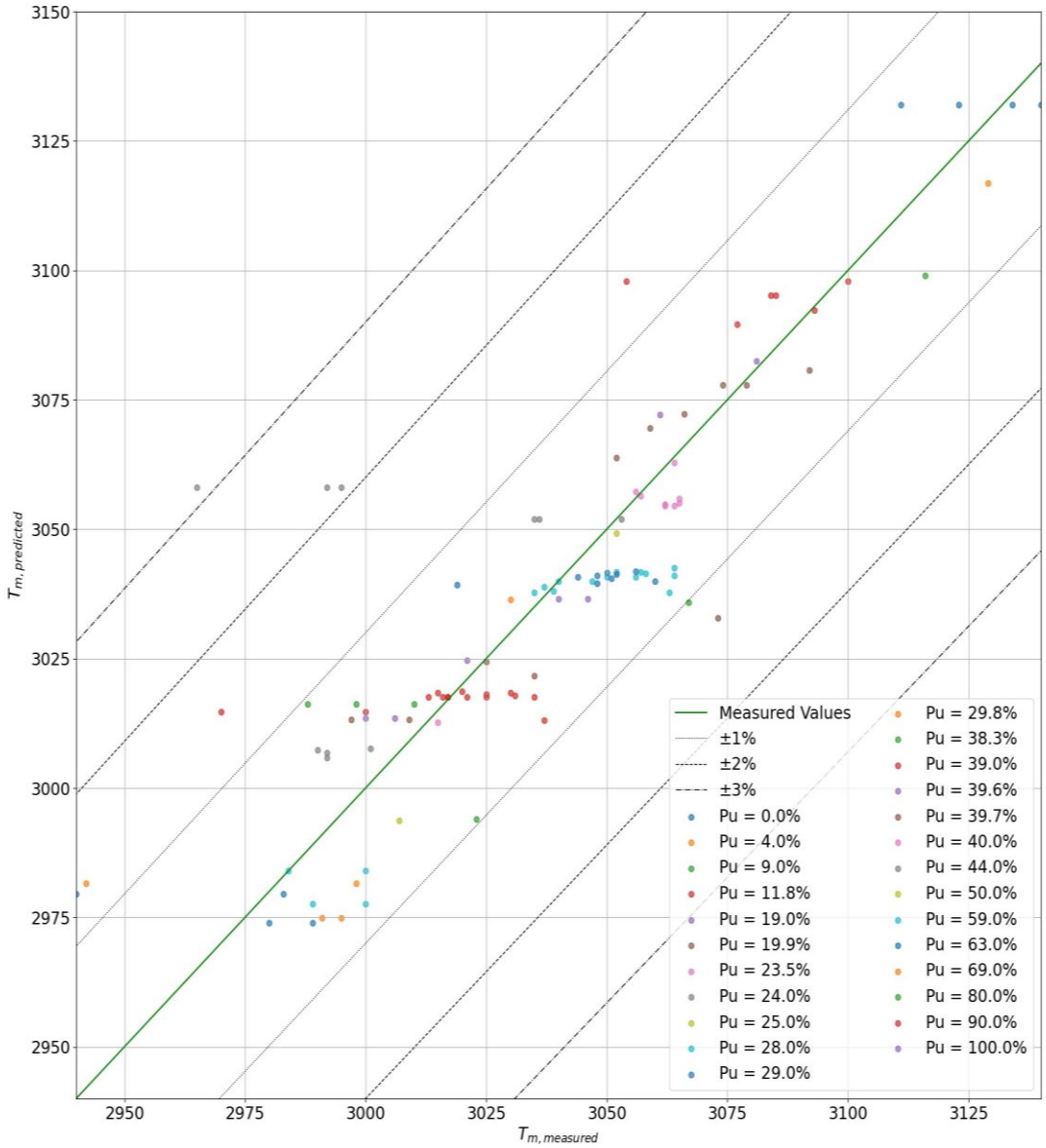

This project has received funding from the Euratom research and training programme 2019-2020 under grant agreement No 945022.